Membrane Location of Spin-Labeled Cytochrome *c* Determined by Paramagnetic Relaxation Agents†

Anna Kostrzewa,‡,§ Tibor Páli,‡,|| Wojciech Froncisz,§ and Derek Marsh*,‡

Max-Planck-Institut für biophysikalische Chemie, Abt. Spektroskopie, D-37070 Göttingen, Germany, and Uniwersytet Jagiellonski, Instytut Biologii Molekularnej, ul. Mickiewicza 3, 31-120 Kraków, Poland

Received November 5, 1999; Revised Manuscript Received February 10, 2000

ABSTRACT: The mitochondrial protein horse heart cytochrome *c* was specifically spin-labeled with succinimidyl-2,2,5,5-tetramethyl-3-pyrroline-1-oxyl-carboxylate on different lysine residues at positions 86, 87, 72, 8, or 25, respectively. Site-specifically labeled species were separated chromatographically and identified by peptide sequencing of tryptic digests. The monolabeled protein was bound to negatively charged phospholipid membranes composed of dioleoylphosphatidylglycerol, and the accessibility of the spin-labeled lysine residues to lipid-soluble molecular oxygen and to lipid-impermeant chromium maltolate was determined from the saturation properties of the ESR spectra. The accessibilities of the spin-labeled proteins relative to those obtained for phospholipids spin-labeled in the headgroup region, in the presence of unlabeled protein, identify the position of the spin-labeled lysine residues relative to the phospholipid bilayer surface. We have found that cytochrome *c* does not penetrate into the membrane interior and that the active side of cytochrome *c* in the protein−membrane interaction is the side on which lys86, lys87, and lys72 are located.

Eukaryotic cytochrome *c* is a soluble electron-transfer protein found in the intermembrane space between the outer and inner membranes of mitochondria. It carries electrons from various dehydrogenase systems to cytochrome *c* oxidase prior to reduction of molecular oxygen and participates in one of the final steps of the terminal respiratory chain that is coupled to oxidative phosphorylation (*1*). Cytochrome *c* is a small, basic, heme-containing protein encoded by the nuclear genome (*2*). The crystal structure of the protein from horse heart (105 residues) has been solved to a resolution of 1.9 Å (*3*), and the most recent solution structure derived from NMR is closely similar, except with respect to the orientation of the surface side chains (*4*). Despite extensive studies, the detailed mechanism of the electron-transfer reactions of cytochrome *c* and its biological redox partners (cytochrome *c* reductase and cytochrome *c* oxidase) is not yet completely understood (see e.g. ref *5*). It is known, however, that electrostatic interactions play a crucial role in these redox processes.

On the basis of kinetic studies using chemically modified cytochrome *c* derivatives, it has been shown that it is the lysine-rich domain around the heme crevice by which cytochrome *c* interacts with the negatively charged binding domains on cytochrome *c* reductase and cytochrome *c* oxidase (*6*, *7*). Results obtained by Vanderkooi and collaborators (*8*) suggest that cytochrome *c* binds to the inner mitochondrial membrane on the side of the protein at which methionine 65 is located. Also, Brown and Wüthrich (*9*) found that membrane-bound cytochrome *c* had a preferred orientation, with the methionine 65 region directed toward the membrane. According to the studies of Muga et al. (*10*), cytochrome *c* does not penetrate the bilayer deeply, and no significant changes in the secondary structure have been found on binding of the protein to negatively charged lipid bilayers (*11*). Binding to lipid membranes does, however, loosen the tertiary folding of cytochrome *c*, as evidenced by increased amide proton exchange rates by a number of techniques (*11*−*13*).

Membrane association of cytochrome *c* has been studied over the pH range from 4 to 7 (*14*). It was found that cytochrome *c* associates electrostatically with acidic phospholipid-containing membranes at neutral pH and, accordingly, is displaced by increasing the ionic strength (*15*). At acidic pH cytochrome *c* was suggested to interact with membrane acidic phospholipids at a further site, presumably by hydrogen bonding. Phosphorus-31 NMR has been used to investigate the interaction of cytochrome *c* with anionic lipid bilayers (*16*, *17*). Disruption of the axial ligation through Met-80 leads to the opening of the heme crevice in the cytochrome *c*, allowing the interaction with the lipid headgroup phosphate (*17*).

Spin-label electron spin resonance (ESR)[1] is capable of providing detailed structural and dynamic information on membrane lipids and proteins (*18*, *19*). The ESR spectra of specifically spin-labeled yeast cytochrome *c* bound to negatively charged DOPG (1,2-dioleoyl-*sn*-glycero-3-phos-

† A.K. was partially supported by the Deutscher Akademischer Austauschdienst. T.P. acknowledges receipt of a short-term fellowship from the Human Frontier Science Program and partial support from the Volkswagen-Stiftung (Germany) and the Hungarian National Science Fundation (OTKA T029458).

* Corresponding author. Tel.: +49-551-201 1285. Fax: +49-551-201 1501. E-mail: dmarsh@gwdg.de.

‡ Max-Planck-Institut.

§ Permanent address: Uniwersytet Jagiellonski, Instytut Biologii Molekularnej, ul. Mickiewicza 3, 31-120 Kraków, Poland.

|| Permanent address: Institute of Biophysics, Biological Research Centre, P.O. Box 521, H-6701 Szeged, Hungary.

10.1021/bi992559l CCC: $19.00
Published on Web 04/27/2000

phoglycerol) bilayers have been studied (*20, 21*). It was found that holocytochrome *c* is associated more intimately with bilayers of the unsaturated anionic lipid DOPG than with those of the saturated DMPG. Despite many different experiments (*13, 16, 20*−*22*) it is still not completely clear what is the degree of penetration of cytochrome *c* into the membrane, which of the residues on the protein are responsible for the interaction of cytochrome *c* with the membrane, and whether cytochrome *c* has a unique orientation when bound to membrane.

In the present work, the location of horse heart cytochrome *c* in association with negatively charged phospholipid bilayer membranes is investigated directly by determining the accessibility of different spin-labeled residues to paramagnetic relaxation agents that are preferentially soluble either in the aqueous phase or in the hydrophobic membrane interior. For this purpose, cytochrome *c* was spin-labeled specifically at various lysine residues located in different regions of the tertiary fold, viz. lys86, lys87, lys72, lys8, or lys25 (*23*). These single modifications of cytochrome *c* by spin-labeling have been found not to affect the conformational characteristics of the cytochrome *c* protein. In parallel, the DOPG membrane was spin-labeled in the lipid headgroup region with a negatively charged phospholipid probe T-PASL (4-phosphatidyl-2,2,6,6-tetramethyl-piperidine-1-oxyl) and the accessibility of the spin-labeled phospholipid to relaxation agents was measured in the presence and absence of cytochrome *c*.

The location of the spin label, attached to the protein (in solution and in the membrane bound form) relative to the membrane−water interface, was determined using paramagnetic quenching quantitated by progressive saturation ESR spectroscopy. This method is based on the exposure of the nitroxide spin label to paramagnetic relaxation agents that are soluble either in the hydrophobic membrane interior, viz., molecular oxygen (*24*−*26*), or in the aqueous phase, viz., chromium maltolate (*27*). Changes in the nitroxide relaxation times due to interactions with the faster relaxing paramagnetic species are a measure of their accessibility to the nitroxide group.

The relaxation agents, molecular oxygen and chromium oxalate, were used earlier to determine the location of bacteriorhodopsin, melittin, apocytochrome *c* and yeast cytochrome *c* in the membrane (*21, 28, 29*). Quite recently, the membrane location of the M13 coat protein was determined by using Ni^{2+} and molecular oxygen as quenching agents (*30*). The disadvantage of the use of chromium oxalate and Ni^{2+}, particularly with charged proteins or charged lipids, is their net electrostatic charges. Use of an uncharged, polar relaxation agent as a probe for the aqueous phase helps to overcome this problem. In this study, chromium maltolate (*27*) was used for this purpose and was found to display a decreasing gradient of concentration from the aqueous phase to the membrane surface, in the presence of bound cytochrome *c*.

[1] Abbreviations: DMPG, 1,2-dimyristoyl-*sn*-glycero-3-phosphoglycerol; DOPG, 1,2-dioleoyl-*sn*-glycero-3-phosphoglycerol; T-PASL, 4-phosphatidyl-2,2,6,6-tetramethylpiperidine-1-oxyl; HEPES, 4-(2-hydroxyethyl)-1-piperazineethanesulfonic acid; TPX, tetramethylpentene polymer; ESR, electron spin resonance; HPLC, high-pressure liquid chromatography; FPLC, fast protein liquid chromatography; TFA, trifluoroacetic acid.

EXPERIMENTAL PROCEDURES

Materials. Cytochrome *c* from horse heart (type VI) was obtained from Sigma (St. Louis, MO), and the spin label succinimidyl-2,2,5,5-tetramethyl-3-pyrroline-1-oxyl-carboxylate was from Molecular Probes (Eugene, OR). Dioleoyl phosphatidylglycerol (DOPG) was obtained from Avanti (Birmingham, AL). Phosphatidic acid spin-labeled at the phosphate of the lipid headgroup 4-phosphatidyl-2,2,6,6-tetramethyl-piperidine-1-oxyl (T-PASL) was prepared essentially according to the method of Eibl (*31*). $Cr(maltolate)_3$ was synthesized as described in ref *27*.

Preparation of Spin-Labeled Cytochrome c Derivatives. The reaction of spin-labeled succinimide with horse heart cytochrome *c* was carried out for 1 h at room temperature in a 2:1 mixture of 10 mM sodium phosphate buffer, pH 5.0, and acetonitrile. The final concentration of cytochrome *c* in the reaction mixture was 8 mg/mL. A few drops of 0.1 M potassium ferricyanide were added to keep the protein in the oxidized state. Equimolar amounts of spin label and protein were used. The initial separation of spin-labeled cytochrome *c* monoderivatives was made by FPLC (Pharmacia/LKB, Malmö, Sweden) on a HR5/5 Mono S column. A 10 mM sodium phosphate pH 7.0 solution was used as an elution buffer with a linear gradient running from 0 to 250 mM NaCl in 60 min (flow rate 1 mL/min). The derivatives for which the cytochrome *c*/spin label ratio was assayed to be 1:1 mol/mol were further purified by HPLC (Pharmacia LKB) using a 250 mm × 4.6 mm SynChropack CM 300 column (SynChrom Inc., Lafayette, IN). A linear gradient running from 0 to 60% of solvent B (solvent A, 30 mM sodium phosphate pH 7.8; solvent B, 300 mM sodium phosphate pH 7.8) with a flow rate of 1 mL/min was used. The concentration of the modified protein was estimated spectrophotometrically (absorbance coefficient $\epsilon = 9.4\ mM^{-1}\ cm^{-1}$, for oxidized cytochrome *c*) using a Beckman DU-7 spectrophotometer. The concentration of spin label bound to cytochrome *c* was estimated from double integration of the first-derivative ESR spectrum, with an aqueous solution of free spin label of known concentration used as a standard. For determination and identification of attachment sites, each purified monoderivative was denatured and resuspended in 0.2 M ammonium bicarbonate buffer pH 8.0 containing 0.1 mM $CaCl_2$ and then digested with TPCK trypsin for 20 h at 37 °C (enzyme/protein ratio 5:100 w:w). Peptides were separated by reverse-phase HPLC (Pharmacia LKB) on a 3.9 × 300 mm Bondapak phenyl column (Waters Associates, Milford, MA) using a linear gradient running from 0 to 50% of solvent B (solvent A, 0.09% TFA in H_2O; solvent B, TFA/H_2O/CH_3CN, 0.09:9.91:90 v:v:v) in 90 min with a flow rate of 0.8 mL/min. After lyophilization of each collected peptide, the presence of spin label was assayed by ESR measurement. The final analysis of the isolated, pure, spin-labeled peptides was made using amino acid sequencing and mass spectrometry in order to identify the positions of the modified lysine residues (*23*).

ESR Sample Preparation. All experiments were performed in a buffer containing 10 mM HEPES pH 7.0. For experiments in the absence of oxygen, buffers were saturated with argon; sample tubes and ESR capillaries were flushed with argon as well. For oxygenated samples, oxygen was flushed around the samples in TPX capillaries (for 1 h) and sample

tubes and ESR capillaries were also flushed with oxygen. Excess supernatant and sample were removed from the membrane pellets in the ESR capillaries to obtain samples ≤ 5 mm in length, so as to avoid inhomogeneities of the microwave and modulation fields in the ESR cavity (cf. ref *32*).

For preparation of lipid dispersions, a dry lipid film was prepared from DOPG (ranging from 0.2 to 0.5 mg) with 0.1 mol % butylated hydroxytoluene to prevent lipid peroxidation. For samples with unlabeled cytochrome *c*, a dry lipid film was prepared from 0.5 mg of DOPG and 1 mol % spin-labeled lipid (T-PASL) with 0.1 mol % butylated hydroxytoluene. The dry lipid film was then hydrated with respectively 100 or 200 μL of buffer and put through 5 cycles of freezing and thawing. After incubation at 37 °C for 30 min, the samples were concentrated by centrifugation (Beckman L7-55, Ti-50 rotor, 50 000 rpm) for 2 h and transferred to 1-mm i.d. glass capillaries. For lipid−protein samples, protein solution was added to the lipid dispersion at a protein/lipid ratio of 1:1 w/w. The samples were incubated for 30−40 min at 37 °C, and the resulting protein−lipid complexes were collected by ultracentrifugation (Beckman L7-55, Ti-50 rotor, 50 000 rpm) for 2 h. Where required, the argonated lipid−protein complexes were resuspended in 17.5 mM $Cr(malt)_3$ freshly dissolved in argonated buffer. Subsequently, the samples were collected by centrifugation for 2 h and transferred to 1-mm i.d. ESR glass capillaries. Samples containing only spin-labeled cytochrome *c* solutions were flushed with oxygen or argon and transferred to 1-mm i.d. ESR capillaries (sample length ≤ 5 mm).

After the ESR measurements, the lipid−protein complexes were dissolved in 40 μL 5% sodium dodecyl sulfate dissolved in 0.5 M NaOH. The phospholipid concentration was determined by the method of Eibl and Lands (*33*), and the protein content was assayed according to the modified method of Lowry (*34*), with bovine serum albumin as standard.

ESR Spectroscopy. ESR spectra were recorded on a Varian Century Line Series 9 GHz spectrometer (Varian Associates, Palo Alto, CA) equipped with nitrogen gas-flow temperature regulation system. The spectrometer was interfaced to an IBM PC to allow signal averaging and digital data storage and analysis. The sample capillaries were accommodated within standard 4 mm quartz ESR tubes containing light silicone oil for thermal stability. Conventional first harmonic, in-phase, absorption spectra were recorded at a modulation frequency of 100 kHz and modulation amplitude of 0.5 G pp, at microwave field amplitudes over the range $\langle H_1^2\rangle^{1/2} = 0.005-0.6$ G for progressive saturation measurements. The H_1-microwave field was calibrated according to ref *32*.

Low-power, conventional ESR spectra were recorded at a subsaturating microwave amplitude corresponding to $\langle H_1^2\rangle^{1/2} = 0.083$ G, for detailed line shape analysis. All measurements were performed under critical coupling conditions. The scan range for low-power spectra was 100 G (using a field/frequency-lock) and 160 G in progressive saturation experiments. Saturation curves were obtained for the total spectral intensity (i.e., the second integral of the first-derivative ESR spectrum) as a function of the root-mean-square microwave magnetic field, $\langle H_1^2\rangle^{1/2}$, for each sample (*35*).

Evaluation of Relaxation and Rotational Rates. The low-power conventional ESR spectra were first integrated and were then fitted to a sum of three Lorentzian absorption line shapes at field positions fixed by the corresponding peak centers. (Note that fitting the absorption spectra, rather than the first-derivative spectra, emphasizes the major component, at the expense of a minor sharp component that is present in some of the spectra; cf. ref *23*.) The fitted line widths were used to calculate transverse relaxation times, T_{2,m_I}, for the three individual m_I hyperfine lines ($m_I = 0, \pm 1$). Finally, a nonlinear least-squares fit to the microwave saturation of the second integrals of the conventional ESR spectra was performed according to the following dependence on H_1 (*35*):

$$I(H_1) = I_0 H_1 \left[\frac{1}{\sqrt{1 + \gamma_e^2 H_1^2 T_1 T_{2,+1}}} + \frac{1}{\sqrt{1 + \gamma_e^2 H_1^2 T_1 T_{2,0}}} + \frac{1}{\sqrt{1 + \gamma_e^2 H_1^2 T_1 T_{2,-1}}} \right] \quad (1)$$

where the common spin−lattice relaxation time, T_1, and normalization factor, I_0, are the two fitting parameters. Rotational diffusion coefficients were obtained from the m_I dependence of the line widths (T_{2,m_I}^{-1}) of the individual hyperfine components according to refs *36* and *37*:

$$1/T_{2,m_I} = A + Bm_I + Cm_I^2 \quad (2)$$

which yields the separate line width coefficients B and C. The latter are directly related to the rotational correlation times, τ_{20} and τ_{22} (*37, 38*):

$$\tau_{20}^{-1} = 6D_{R\perp} \quad (3)$$

$$\tau_{22}^{-1} = 2D_{R\perp} + 4D_{R\parallel} \quad (4)$$

where $D_{R\parallel}$, $D_{R\perp}$ are the axial and off-axial components of the diffusion tensor. Alternatively, if the rotational diffusion is near to isotropic, the effective diffusion coefficient for isotropic rotation, D_R^{eff}, can be obtained from the relative Lorentzian broadening of the $m_I = 0$ and $m_I = -1$ manifolds, i.e., from $B + C$ in eq 2. The corresponding isotropic rotational correlation time is then $\tau_R = (6D_R^{eff})^{-1}$.

RESULTS

Spin-Labeled Cytochrome c in Buffer. The ESR spectra of cytochrome *c* spin-labeled on the different lysine groups are given in Figure 1. The spectra of free cytochrome *c* in buffer solution are those given by the solid lines. For comparison, the ESR spectrum of the headgroup-labeled phospholipid, T-PASL, in bilayer membranes of DOPG is also included in this figure. With the exception of the label on lys72, the ESR spectra of spin-labeled cytochrome *c* in buffer consist of three sharp, differentially broadened ^{14}N-hyperfine lines. The mean rotational diffusion coefficients, $D_{\bar{R}} = (D_{R\parallel}D_{R\perp})^{1/2}$ (*38*), of the free cytochrome *c* spin labels were determined from the Lorentzian line widths as described under Experimental Procedures and are given in Table 1. To allow for any anisotropy in the rotational diffusion, the diffusion coefficients for axial ($D_{R\parallel}$) and off-axial ($D_{R\perp}$) rotation were obtained separately by using the relative widths of all three hyperfine lines (*37*). The anisotropy in rotational diffusion, $D_{R\parallel}/D_{R\perp}$, and the effective rotational diffusion

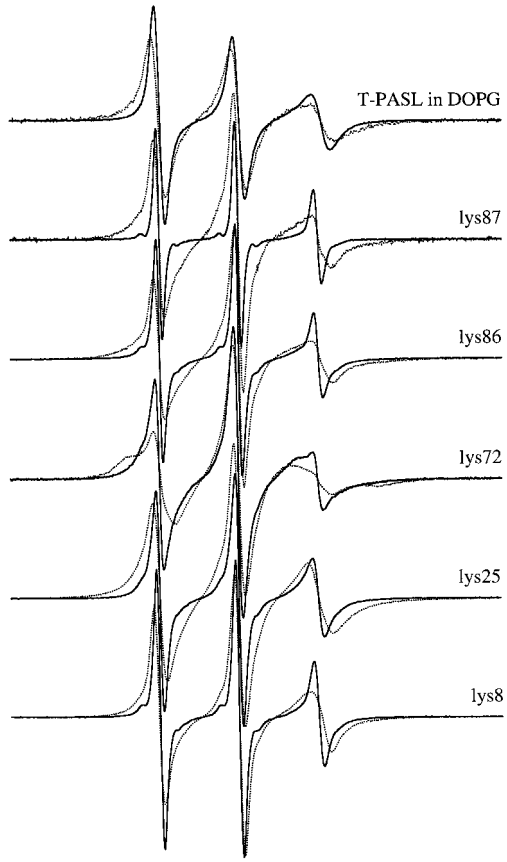

FIGURE 1: Low-power conventional ESR spectra of T-PASL in DOPG with (dotted line) and without (solid line) cytochrome *c* and the ESR spectra of specifically spin-labeled monoderivatives of cytochrome *c* free in solution (solid lines) and bound to DOPG membranes (dotted lines). The lysine residue on cytochrome *c* that is spin-labeled is indicated in the figure. Modulation amplitude, total scan width, and temperature are 0.5 G, 100 G, and 30 °C, respectively.

Table 1: Rotational Diffusion Coefficients (D_R^{eff}, $D_{\bar{R}}$), Rotational Anisotropies ($D_{R//}/D_{R\perp}$), and Changes in the Spin−Lattice Relaxation Rate $\Delta(1/T_1)$ Due to Oxygen, for Spin-Labeled Monoderivatives of Cytochrome *c* in Buffer and for T-PASL in DOPG, Measured at 30 °C

sample	D_R^{eff} (10^8 s^{-1})	$D_{\bar{R}}$ (10^8 s^{-1})	$D_{R//}/D_{R\perp}$	$\Delta(1/T_1)(O_2)$ (10^6 s^{-1})
T-PASL in DOPG	1.3	2.1	11	0.40 ± 0.12
lys87 in buffer	2.5	2.6	0.22	0.77 ± 0.26
lys86 in buffer	1.5	1.6	1.0	3.74 ± 0.28
lys72 in buffer	0.7	0.7	2.7	1.93 ± 0.32
lys25 in buffer	1.5	1.5	1.1	4.04 ± 0.18
lys8 in buffer	2.1	2.3	1.8	0.87 ± 0.22

coefficients, D_R^{eff}, calculated assuming isotropic rotation, are also included in Table 1.

The diffusion coefficient for overall rotation of the cytochrome *c* molecule in buffer is given by the Debye equation (*39*):

$$D_{\bar{R}}^{\circ} = kT/(6\pi\eta\bar{\nu}) \quad (5)$$

Here η is the aqueous viscosity and $\bar{\nu}$ is the partial specific volume of cytochrome *c*. At 30 °C in buffer, $D_{\bar{R}}^{\circ} = 0.6 \times 10^8$ s^{-1}, a value which is close to the mean rotational diffusion coefficient measured for cytochrome *c* spin-labeled on lys72. In the latter case, the spin label has little

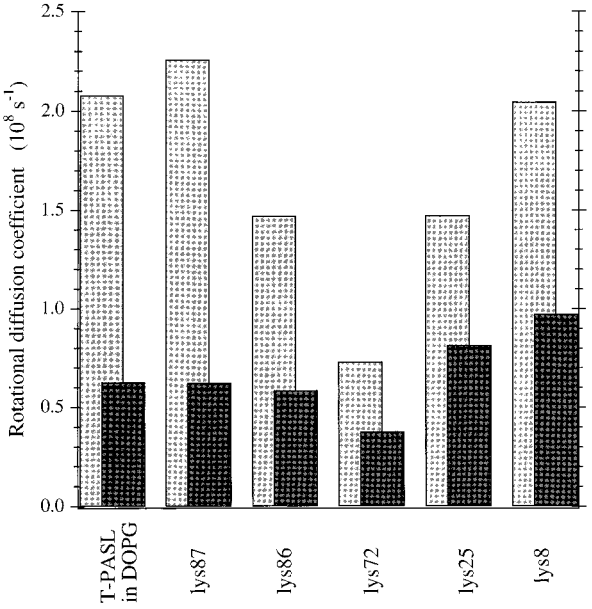

FIGURE 2: Rotational diffusion coefficients, $D_{\bar{R}}$, measured for T-PASL in DOPG without (gray bar) and with (dark bar) cytochrome *c* and for spin-labeled monoderivatives of cytochrome *c* free in solution (gray bars) and bound to DOPG membranes (dark bars). The lysine residue on cytochrome *c* that is spin-labeled is indicated in the figure. Temperature = 30 °C.

independent motion relative to the whole protein, whereas for all other positions of lysine labeling the spin label attachment displays considerable additional segmental motion. Assuming additivity of diffusional rates one can therefore write:

$$D_{\bar{R}} = D_{\bar{R}}^{\circ} + D_{\bar{R},seg} \quad (6)$$

where $D_{\bar{R}}^{\circ}$ represents overall rotation of the protein and $D_{\bar{R},seg}$ represents the segmental rotation of the spin label relative to the protein backbone. The greatest values of $D_{\bar{R},seg}$ are for the labels on lys87 toward the C-terminal and on lys8, close to the N-terminal. The membrane-bound T-PASL displays preferential anisotropic motion about the spin label *x*-axis (cf. refs *36* and *37*).

Spin-Labeled Cytochrome c Bound to Lipid. The ESR spectra of the spin-labeled cytochrome *c* derivatives bound to DOPG membranes and of the spin-labeled phospholipid T-PASL in the presence of unlabeled cytochrome *c* are also given in Figure 1 (dotted lines). A decrease in rotational mobility of the spin label on binding cytochrome *c* to the membranes is evident in all cases. The rotational diffusion coefficients for each spin label with protein in the bound and unbound states are given in Figure 2. In the bound state, the spin label on lys8 has the greatest mobility, followed by that of the spin label on lys25. The spin label on lys72 is rather strongly immobilized on membrane binding. Its spectrum is approaching the slow motional regime of spin label ESR spectroscopy for which $D_{\bar{R}} \sim 0.1 \times 10^8$ s^{-1} (see Figure 1). This corresponds to immobilization of the overall protein rotation on membrane binding, because the spin label on lys72 has little segmental mobility, even for the unbound protein. Of the labels with independent segmental mobility in buffer, the largest change, $\Delta D_{\bar{R}}$, in rotational diffusion coefficient on membrane binding is for the spin label on lys87, whereas the smallest change is for the spin label on

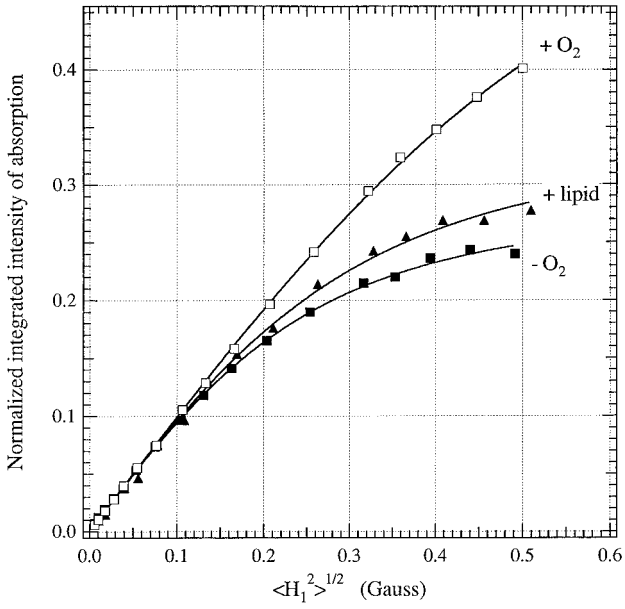

FIGURE 3: Progressive saturation curves for the second integral of the conventional ESR spectra, for cytochrome *c* spin-labeled on lys86: free in deoxygenated solution (solid squares); bound to deoxygenated DOPG membranes (triangles); bound to DOPG membranes saturated with oxygen (open squares). The integrated ESR intensity is plotted against the root-mean-square microwave magnetic field intensity, $\langle H_1^2\rangle^{1/2}$, at the sample, and is normalized to the same slope at low power. Other experimental conditions are as for Figure 1. Solid lines are nonlinear least-squares fits of eq 1 to the saturation curves.

lys25. In the latter case, $\Delta D_{\bar{R}} \approx D_{\bar{R}}^{\circ}$; i.e., essentially only the contribution from overall rotation of the protein is suppressed and the segmental mobility of the spin label on lys25 remains essentially unaffected by binding to the membrane. For all other lysine groups spin-labeled, membrane binding additionally induces a decrease in segmental mobility, most prominently for lys87 which presumably therefore directly contacts the membrane surface.

The rotational mobility of the T-PASL lipid, spin-labeled in the polar group region, is greatly reduced by binding cytochrome *c* to DOPG membranes. This is consistent with a direct steric interaction between cytochrome *c* and spin labels at the lipid polar headgroups, on protein binding to the membrane surface.

The spin−lattice relaxation enhancements by molecular oxygen have been determined for the various spin labels in solution by methods to be described later. These values are also included in Table 1 but do not correlate directly with the spin label rotational mobilities that are presented in the table.

Progressive Saturation Studies: Lipid/Protein Interaction. Typical saturation curves with increasing microwave power are shown for spin-labeled cytochrome *c* in Figure 3. Binding of spin-labeled cytochrome *c* to DOPG membranes decreases the degree of saturation, giving rise to larger spectral intensities at high microwave power (compare solid squares and triangles in Figure 3). Results from the sample in oxygen (open squares in Figure 3) indicate, however, that useful sensitivity to the presence of paramagnetic relaxation agents still remains after membrane binding.

Values of the effective T_1T_2 relaxation time product obtained for the different spin-labeled cytochrome *c* derivatives in the presence and absence of DOPG membranes are given in Table 2. These values were obtained by fitting a single component model to the saturation curves, i.e., by assuming that $T_{2,+1} = T_{2,0} = T_{2,-1}$ in eq 1. Corresponding values for the headgroup-labeled T-PASL lipid in DOPG membranes, in the presence and absence of unlabeled cytochrome *c*, are also given in Table 2. In nearly all cases, there is a substantial decrease in the effective T_1T_2 product on binding of cytochrome *c*. The sole exception to this is cytochrome *c* labeled on lys72, for which the rotational broadening of the spectrum is already very considerable when the protein is free in solution. Binding to the membrane, in the latter case, drives the spectrum into the slow motional regime. Spectral simulations that include rotational dynamics of the spin label have been made recently for progressive saturation experiments of the type performed here (*40*). These show that, for spectra in the fast motional regime (such as those here, with the exception of lys72), the T_1T_2 product obtained in progressive saturation experiments decreases with decreasing rotational diffusion coefficient. The decrease in $(T_1T_2)^{\text{eff}}$ in Table 2 is therefore a result of the rotational immobilization on binding cytochrome *c* to the membrane, which is consistent with the line width analysis given above. For cytochrome *c* labeled on lys72, the increase in $(T_1T_2)^{\text{eff}}$ is associated with a transition to the slow motional regime, that is also consistent with theoretical simulations (*40*). For lys8, the values of $(T_1T_2)^{\text{eff}}$ in the free and bound states just overlap, within the error range. However, there is an apparent tendency for the T_1T_2 product to increase on binding. It is possible that there are intrinsic increases in T_1 with decreasing rotational mobility that are not included explicitly in the theoretical simulations (*40*), which were based solely on rotational modulation of the spectral anisotropies.

Table 2: Values of the Effective T_1T_2 Relaxation Time Products for Different Monoderivatives of Spin-Labeled Cytochrome *c* Free in Solution and Bound to DOPG Membranes, and for T-PASL in DOPG Membranes with and without Cytochrome *c*

sample	T_1T_2 in buffer (10^{-14} s^2)	T_1T_2 bound (10^{-14} s^2)
T-PASL in DOPG	2.24 ± 0.06	2.13 ± 0.14
lys87	4.72 ± 0.46	1.48 ± 0.32
lys86	3.94 ± 0.18	2.73 ± 0.22
lys72	1.36 ± 0.07	1.63 ± 0.09
lys25	3.76 ± 0.11	2.05 ± 0.03
lys8	2.51 ± 0.06	2.82 ± 0.25

Further analysis, by measuring the individual hyperfine line widths and fitting eq 1 to the saturation curves, as described in Experimental Procedures, was also performed. This leads to values for the T_1 relaxation times, in the presence and in the absence of cytochrome *c* binding to the membranes. These results are given in Figure 4. It is seen that the T_1 relaxation rate either decreases, or does not change significantly (lys25, lys87), on binding of cytochrome *c* to the DOPG membranes. For rotational rates that are below the Larmor frequency ($\sim 5 \times 10^{10}$ s^{-1}), the spin−lattice relaxation rate is both expected and observed to decrease with decreasing rotational diffusion coefficient (see e.g. ref *41*). The results of Figure 4, therefore, are also consistent with the rotational immobilization on membrane binding of cytochrome *c*.

Progressive Saturation: Relaxation Agents. Typical saturation curves for spin-labeled cytochrome *c* in the presence

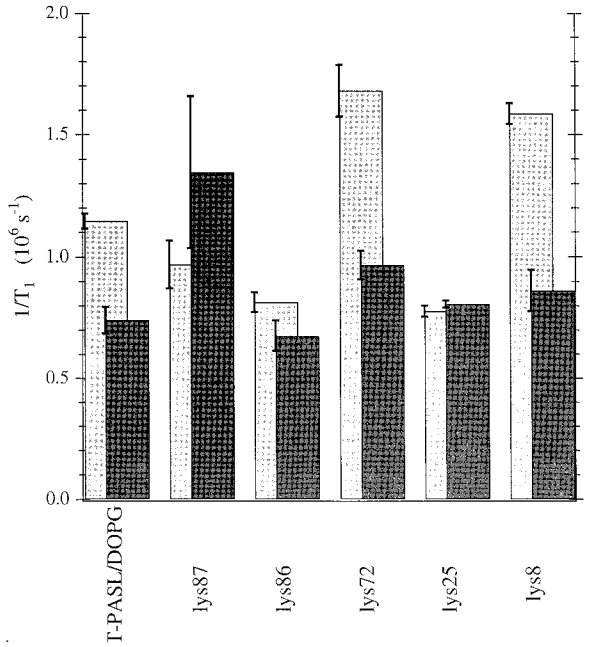

FIGURE 4: Spin−lattice relaxation rates ($1/T_1$) for T-PASL in DOPG and for spin-labeled monoderivatives of cytochrome *c* either free in solution (gray bars) or bound to DOPG membranes (black bars), measured at 30 °C. All samples are deoxygenated.

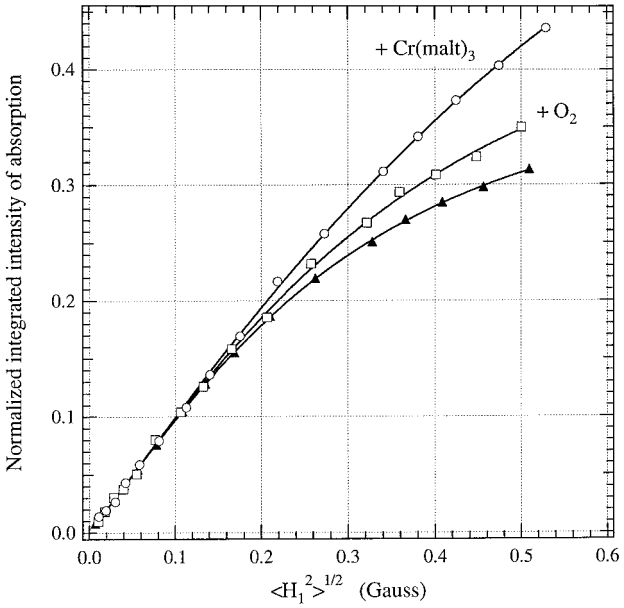

FIGURE 5: Progressive saturation curves for the normalized integrated intensity of the ESR absorption from cytochrome *c* spin-labeled on lys25 and bound to DOPG membranes, with no relaxant (triangles) and in the presence of molecular oxygen (squares) or 17.5 mM $Cr(malt)_3$ (circles). Temperature = 30 °C. Solid lines are nonlinear least-squares fits of eq 1 to the saturation curves.

of polar and apolar paramagnetic relaxation agents are given in Figure 5. Oxygen, as an apolar paramagnetic relaxant, partitions preferentially into the hydrophobic interior of the lipid membrane. Chromium maltolate, as a polar relaxant, dissolves preferentially in the aqueous phase. Of the various paramagnetic ions and their complexes tested, $Cr(malt)_3$ was found more appropriate for the present studies with charged proteins and membranes, because of its lack of electrostatic charge and relatively low partition coefficient into membranes.

Table 3: Increases in Relaxation Rate Products, $\Delta(1/T_1T_2)$, Measured at 30 °C, as a Result of Oxygen- and $Cr(malt)_3$-Induced Relaxation Enhancement of Spin-Labeled Cytochrome *c* Derivatives Associated with DOPG Membranes and with Spin Labels Located in the Headgroup Region in the Membrane (T-PASL)

sample	$\Delta(1/T_1T_2)(O_2)$ (10^{14} s^{-2})	$\Delta(1/T_1T_2)(Cr(malt)_3)$ (10^{14} s^{-2})
T-PASL in DOPG with cyt *c*	1.16 ± 0.13	0
lys86	1.10 ± 0.11	1.02 ± 0.08
lys72	0.27 ± 0.12	1.07 ± 0.11
lys25	0.24 ± 0.05	1.37 ± 0.12
lys8	0.17 ± 0.06	1.49 ± 0.21

Figure 5 shows that the two relaxation agents alleviate saturation of cytochrome *c* spin-labeled on lys25 to differential extents, when the protein is bound to DOPG membranes. Relaxation enhancement by $Cr(malt)_3$ is much more efficient than that by molecular oxygen. Increases, $\Delta(1/T_1T_2)$, in the reciprocal T_1T_2 relaxation time product that are induced by the two paramagnetic relaxants were determined from the saturation curves, as described above. These results are given in Table 3 for the different spin-labeled derivatives of cytochrome *c* bound to DOPG membranes and also for T-PASL in DOPG membranes to which unlabeled cytochrome *c* is bound. The largest effect of oxygen is found in the lipid headgroup region for T-PASL and for cytochrome *c* spin-labeled on lys86. For cytochrome *c* labeled on lys72, lys25, or lys8, the oxygen effect is very low, about five times less. In contrast, the effect of $Cr(malt)_3$ is large for spin-labeled lys8 and lys25 and smaller for spin-labeled lys72 and lys86. For T-PASL, no effect of $Cr(malt)_3$ is observed, presumably because binding of cytochrome *c* at saturation surface coverage prevents access of this bulkier relaxation agent to the lipid headgroups. (In the absence of protein, $Cr(malt)_3$ induces an approximately 50−60% increase in $(T_1T_2)^{eff}$ of T-PASL, i.e., $\Delta(1/T_1T_2) \approx -1.5 \times 10^{13}$ s^{-2}, presumably because of direct association with the polar surface of DOPG membranes.) These reciprocal differential effects of the two complementary relaxation agents demonstrate a high degree of spatial discrimination in this system.

The paramagnetic effects of the relaxation agents on the T_1T_2 product are modulated by the differences in line widths of the different spin-labeled species (cf. Figure 1 and Tables 1 and 2). A less biased comparison can be made by using the spin−lattice relaxation rate enhancements, $\Delta(1/T_1)$, because the individual spin-label T_1 relaxation rates are all very similar in the membrane-bound form, in the absence of relaxation agents (see Figure 4). The values of $\Delta(1/T_1)$ induced by molecular oxygen and 17.5 mM $Cr(malt)_3$ were determined by line width measurements and fitting the saturation curves to eq 1, as described in Experimental Procedures. These results are given in Figure 6. A very clear differentiation is seen between the relative effects of the two complementary relaxation agents that is consistent with lys86, and to a less decisive extent lys72, being located facing the phospholipid headgroups. Lys25 and lys8, on the other hand, are exposed to the aqueous phase as indicated by their high exposure to $Cr(malt)_3$ and the fact that they experience a low concentration of oxygen.

DISCUSSION

Cytochrome c in Solution. The different segmental mobilities of the various spin-labeled lysine residues of cytochrome

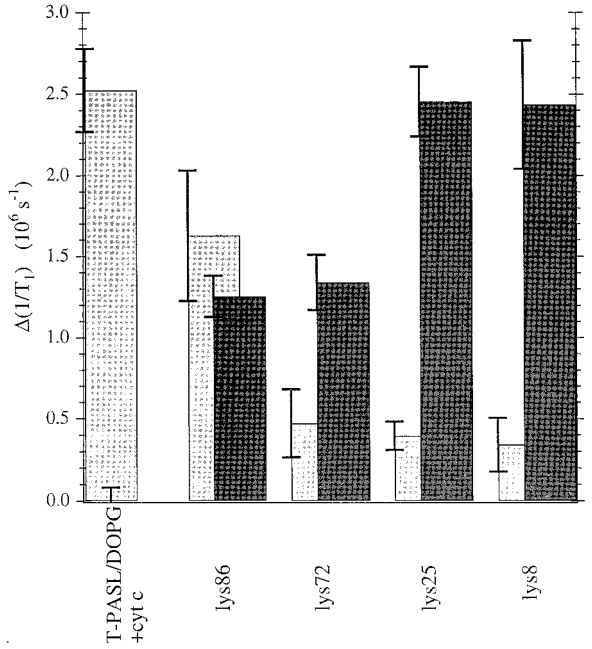

FIGURE 6: Increases in the spin−lattice relaxation rate $\Delta(1/T_1)$ induced by oxygen (gray bars) and 17.5 mM $Cr(malt)_3$ (black bars). Effects were measured at 30 °C for membrane-bound cytochrome *c* with the spin label located at lys86, lys72, lys8, or lys25 or in the phospholipid headgroup region (T-PASL).

c free in solution might be expected to reflect the local environment of these residues. Most strikingly, the spin label on lys72 appears to have little segmental mobility, although the lysine residues are located at the protein surface. Comparison with the crystal structure has shown previously that this residue is in the most crowded region of the residues investigated and is also closest to the haem group (*23*). It is noteworthy that the spin label on lys72 is also that which displays the greatest rotational anisotropy. This again is indicative of a relatively close-packed environment.

The accessibility of the spin-labeled lysine residues to oxygen dissolved in solution (see Table 1) does not correlate directly with the rotational mobility of the labels. It is likely that the values of $\Delta(1/T_1)$ that are given for oxygen as relaxant in Table 1 reflect local variations in oxygen concentration over the surface of the protein, rather than intrinsic accessibility. This again points to a heterogeneity in the local environment of the different lysine residues labeled.

Orientation of Membrane-Bound Cytochrome c. As already discussed in Results, the effects of membrane binding on the segmental mobility of the labeled residues indicate that the protein surface bearing lys87 is that which interacts with the membrane. Spin-labeled residues located on this surface have the lowest rotational diffusion coefficients in the bound state (Figure 2). With the exception of lys86, they also have the lowest values of the effective T_1T_2 product (Table 2) and of spin−lattice relaxation time (Figure 4), in the bound state.

Measurements of the differential relaxation enhancements by oxygen and $Cr(malt)_3$ reinforce this interpretation. The proposed orientation of cytochrome *c* bound to DOPG membranes that is deduced from the relaxation enhancements is indicated in Figure 7. Spin labels on those residues proposed to be facing the membrane surface have larger relaxation enhancements induced by molecular oxygen, and smaller ones induced by $Cr(malt)_3$, just as for the surface-located lipid spin label T-PASL (see Table 3 and Figure 6). Correspondingly, spin labels on residues at the opposite face of cytochrome *c*, which is proposed to be facing the aqueous phase, experience larger relaxation enhancements by $Cr(malt)_3$ and smaller ones by molecular oxygen. This consistent degree of discrimination between the effects of the two relaxation agents suggests that their concentration gradients increase in opposite directions at the membrane surface, when protein is bound. In the case of $Cr(malt)_3$, the gradient arises at least in part from steric restrictions, because this relaxant produces little change for T-PASL, when the membrane surface is saturated with cytochrome *c* (Figure 6). In this connection, it should be noted that the spin label has a very short link to the lipid headgroup in T-PASL, unlike that for the label attached to lysine which already has a relatively long and flexible side chain. For oxygen, the concentration profile is most probably determined by the gradient of polarity at the membrane surface, with preferential enrichment of relaxant in the more apolar regions. These two effects contribute materially to the success of the method and are likely to operate generally and to prove useful for studies on other similar systems. This method differs, in principle, from the general procedure developed recently for determining protein orientation at charged membrane surfaces by combining charged relaxants with electrostatic calculations (*42*).

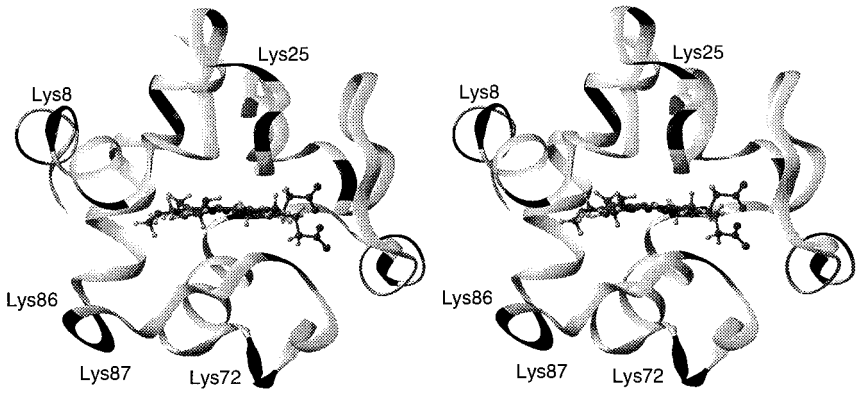

FIGURE 7: Orientation of cytochrome *c* bound to DOPG membranes. The membrane surface is located at the bottom of the figure. Lysine residues are represented by dark bands on the ribbon diagram, and those that have been spin-labeled are numbered. Those at the top face of cytochrome *c* experience the largest paramagnetic relaxation enhancements by $Cr(malt)_3$ and the lowest by molecular oxygen, and vice-versa for the residues at the bottom face of the protein. The protein structure is that of ref *4* (PDB accession number, 1AKK).

The membrane orientation of cytochrome *c* that is given in Figure 7 is consistent, at least qualitatively, with previous measurements of cytochrome *c* binding in other membrane systems. A preferential immobilization of a spin label on met65 relative to cys103 was found for cytochrome *c* bound to mitochondrial membranes (*8*). Paramagnetic relaxation enhancement of the lipid ^{1}H NMR resonances suggests that a spin label on met65 of cytochrome *c* contacts the membrane surface of cardiolipin-containing lipid vesicles (*9*). Met65 is located on the same surface of cytochrome *c* as lys86, lys87, and lys72. The orientation of the haem plane of cytochrome *c* bound to mitochondrial membranes was found to be different from that of the hemes in cytochrome *c* oxidase (*43*), which are known to lie approximately perpendicular to the membrane plane (*43*, *44*).

It is noted that the degree of consistency in the results obtained from the different labeling positions indicates that modifying a specific lysine does not alter the mode of association of cytochrome *c* with the membrane. The whole protein contains a total of 21 positively charged residues (19 lysines and 2 arginines). Therefore, removing the charge of a single lysine on labeling is likely to have little effect on the overall electrostatic-driven association with negatively charged membranes.

Location of Membrane-Bound Cytochrome c. As noted in the Introduction, there has been some controversy regarding whether cytochrome *c* partially penetrates into DOPG membranes or is simply bound to the surface as for classical peripheral proteins. The ESR spectra of spin labels that are attached to different lysine groups on the surface of cytochrome *c* are partially, but not strongly, immobilized on binding to DOPG, relative to the situation free in solution. Compared with the anisotropic ESR spectra of lipids labeled in the chain regions of fluid lipid membranes, the mobility of the labeled lysine groups is still rather high. Therefore it is unlikely that cytochrome *c* penetrates deeply into DOPG membranes. The reduction in accessibility to $Cr(malt)_3$ is also less for the labeled lysines than that found for the headgroup spin-labeled lipid T-PASL, with cytochrome *c* bound (Figure 6). Therefore, it is likely that cytochrome *c* remains associated at the surface of DOPG membranes. These conclusions are consistent with those of infrared measurements on DOPG membranes, relative to cardiolipin-containing membranes (*22*). They are also consistent with the location of cytochrome *c*, relative to that of apocytochrome *c*, that was suggested both from experiments with paramagnetic relaxation agents and from double labeling experiments involving spin-labeled protein and spin-labeled lipids (*21*, *45*).

In conclusion, the present experiments with uncharged paramagnetic relaxants and site-specific spin labels on the basic protein have demonstrated that cytochrome *c* adopts a preferred orientation when bound to negatively charged membranes of DOPG. This orientation, with the face of cytochrome *c* bearing lys86, lys87, and lys72 directed toward the membrane surface, is fully consistent with the effects of membrane binding on the mobility of the spin-labeled lysine groups. The particular combination of relaxation enhancements used here is likely to prove useful for studies on similar lipid−protein systems, in the future.

ACKNOWLEDGMENT

We thank Frau B. Angerstein for the preparation of chromium maltolate and Drs. A. Watts and H. Eibl for preparation of the spin label T-PASL.

REFERENCES

1. Kar, L., Sherman, S. A., and Johnson, M. E. (1994) *J. Biomol. Struct. Dyn. 12*, 527−558.
2. Moore, G. R., and Pettigrew, G. W. (1990) *Cytochromes c. Evolutionary, Structural and Physicochemical Aspects*, pp 1−227, Springer-Verlag, Berlin, New York, Hong Kong.
3. Bushnell, G. W., Louie, G. V., and Brayer, G. D. (1990) *J. Mol. Biol. 214*, 585−595.
4. Banci, L., Bertini, I., Gray, H. B., Luchinat, C., Reddig, T., Rosato, A., and Turano, P. (1997) *Biochemistry 36*, 9867−9877.
5. Wikström, M. (1998) *Curr. Opin. Struct. Biol. 8*, 480−488.
6. Koppenol, W. H., and Margoliash, E. (1982) *J. Biol. Chem. 257*, 4426−4437.
7. Margoliash, E., and Bosshard, H. R. (1983) *Trends Biochem. Sci. 8*, 316−320.
8. Vanderkooi, J., Erecinska, M., and Chance, B. (1973) *Arch. Biochem. Biophys. 157*, 531−540.
9. Brown, L. R., and Wüthrich, K. (1977) *Biochim. Biophys. Acta 468*, 389−410.
10. Muga, A., Mantsch, H. H., and Surewicz, W. K. (1991) *Biochemistry 30*, 7219−7224.
11. Heimburg, T, and Marsh, D. (1993) *Biophys. J. 65*, 2408−2417.
12. De Jongh, H. H. J., Killian, J. A., and de Kruijff, B. (1992) *Biochemistry 31*, 1636−1643.
13. Spooner, P. J. R., and Watts, A. (1991) *Biochemistry 30*, 3871−3879.
14. Rytömaa, M., Mustonen, P., and Kinnunen, P. K. J. (1992) *J. Biol. Chem. 267*, 22243−22248.
15. Görrissen, H., Marsh, D., Rietveld, A. and de Kruijff, B. (1986) *Biochemistry 25*, 2904−2910.
16. Spooner, P. J. R., and Watts, A. (1991) *Biochemistry 30*, 3880−3885.
17. Pinheiro, T. J. T., and Watts, A. (1994) *Biochemistry 33*, 2451−2458.
18. Marsh, D. (1981) in *Membrane Spectroscopy. Molecular Biology, Biochemistry and Biophysics* (Grell, E., Ed.) Vol. 31, pp 51−142, Springer-Verlag, Berlin, Heidelberg, New York.
19. Hubbell, W. L., and Altenbach, C. (1994) in *Membrane protein structure: experimental approaches* (White, S. H., Ed.) pp 224−248, Oxford University Press, New York.
20. Snel, M. M. E., de Kruijff, B., and Marsh, D. (1994) *Biochemistry 33*, 7146−7156.
21. Snel, M. M. E., de Kruijff, B., and Marsh, D. (1994) *Biochemistry 33*, 11150-11157.
22. Choi, S., and Swanson, J. M. (1995) *Biophys. Chem. 54*, 271−278.
23. Turyna, B., Osyczka, A., Kostrzewa, A., Blicharski, W., Enghild, J. J., and Froncisz, W. (1998) *Biochim. Biophys. Acta 1386*, 50−58.
24. Subczynski, W. K., and Hyde, J. S. (1981) *Biochim. Biophys. Acta 643*, 283−291.
25. Subczynski, W. K., and Hyde, J. S. (1983) *Biophys. J. 41*, 283−286.
26. Subczynski, W. K., and Hyde, J. S. (1984) *Biophys. J. 45*, 743−748.
27. Burchfield, J., Telehowski, P., Rosenberg, R. C., Eaton, S. S., and Eaton, G. R. (1994) *J. Magn. Reson. 104*, 69−72.
28. Altenbach, C., and Hubbell, W. L. (1988) *Proteins 3*, 230−242.
29. Altenbach, C., Froncisz, W., Hyde, J. S., and Hubbell, W. L. (1989) *Biophys. J. 56*, 1183−1191.
30. Stopar, D., Jansen, K. A. J., Páli, T., Marsh, D., and Hemminga, M. A. (1997) *Biochemistry 36*, 8261−8268.
31. Eibl, H. (1978) *Proc. Natl. Acad. Sci. U.S.A. 75*, 4074−4077.

32. Fajer, P., and Marsh, D. (1982) *J. Magn. Reson. 49*, 212−224.
33. Eibl, H., and Lands, W. E. M. (1969) *Anal. Biochem. 30*, 51−57.
34. Peterson, G. L. (1977) *Anal. Biochem. 83*, 346−356.
35. Páli, T., Horváth, L. I., and Marsh, D. (1993) *J. Magn. Reson. A 54*, 363−373.
36. Marsh, D. (1985) in *Spectroscopy and the Dynamics of Molecular Biological Systems* (Bayley, P. M., and Dale, R. E., Eds.) pp 209−216, Academic Press, London.
37. Marsh, D. (1989) in *Biological Magnetic Resonance 8, Spin Labeling Theory and Applications* (Berliner, L. J., and Reuben, J., Eds.) pp 255−303, Plenum Publishing Corp., New York.
38. Goldman, A., Bruno, G. V., Polnaszek, C. F., and Freed, J. H. (1972) *J. Chem. Phys. 56*, 716−735.
39. Marsh, D., and Horváth, L. I. (1989) in *Advanced EPR. Applications in Biology and Biochemistry* (Hoff, A. J., Ed.) pp 707−752, Elsevier, Amsterdam.
40. Livshits, V. A., Páli, T., and Marsh, D. (1998) *J. Magn. Reson. 133*, 79−91.
41. Marsh, D., Páli, T., and Horváth, L. I. (1998) in *Biological Magnetic Resonance, Vol. 14, Spin Labeling. The Next Millenium.* (Berliner, L. J., Ed.) pp 23−82, Plenum Press, New York.
42. Lin, Y., Nielsen, R., Murray, D., Hubbell, W. L., Mailer, C., Robinson, B. H., and Gelb, M. H. (1998) *Science 279*, 1925−1929.
43. Erecinska, M., Blasie, J. K., and Wilson, D. F. (1977) *FEBS Lett. 76*, 235−239.
44. Tsukihara, T., Aoyama, H., Yamashita, E., Tomizaki, T., Yamaguchi, H., Shinzawa-Itoh, K., Nakashima, R., Yaono, R., and Yoshikawa, S. (1996) *Science 272*, 1136−1144.
45. Snel, M. M. E., and Marsh, D. (1994) *Biophys. J. 67*, 737−745.

BI992559L